Current Control of LCL-Filtered Grid-Connected VSC Using Model Predictive Control with Inherent Damping

Nørgaard, Jacob Bitsch; Taul, Mads Graungaard; Dragicevic, Tomislav; Blaabjerg, Frede

Published in:
Proceedings of 2018 20th European Conference on Power Electronics and Applications (EPE'18 ECCE Europe)

Publication date:
2018

Document Version
Accepted author manuscript, peer reviewed version

Current Control of LCL-Filtered Grid-Connected VSC using Model Predictive Control with Inherent Damping

Jacob Bitsch Nørgaard, Mads Kjeldal Graungaard, Tomislav Dragičević, Frede Blaabjerg
Department of Energy Technology, Aalborg University
Pontoppidanstde 111, 9220 Aalborg East, Denmark
Phone: +45 99 40 92 40
Fax: +45 99 40 38 20
Email: jbn@et.aau.dk
URL: http://www.et.aau.dk

Acknowledgments

This research was supported by the REliable Power Electronic based Power System (REPEPS) research project at Aalborg University, Denmark.

Keywords

≪Model Predictive Control≫, ≪Grid-Connected Converter≫, ≪Voltage-Source Converter≫, ≪Nonlinear Control≫, ≪Active Damping≫.

Abstract

The advancement on penetration of renewable energy sources in the power system is, in part, tied to the current control of grid-connected LCL-filtered voltage source converters. A challenge is current control with the addition of the LCL-filter resonance, which interacts with the digital converter-control switching action and creates the possibility for instability. In certain scenarios, active damping is needed to stabilize the system and ensure robust performance in steady-state and dynamic response. Another approach is detailed in this paper where a hybrid linear and nonlinear controller is implemented to ensure the dynamic current control performance. This is done by combining a linear outer-loop Proportional Resonant current controller with a nonlinear inner-loop Model Predictive voltage controller to replace the fixed switching-frequency Pulse Width Modulator. This allows for easy compensation of nonlinear effects, such as time delays and provides the controller with the ability to prioritize the dynamic performance during step changes. The details for implementing this control structure are provided, along with a discussion of the advantages, and guidelines for the design procedure of the hybrid control structure. Simulation results and experimental measurements are provided to illustrate the control performance and validate the proposed method. As a conclusion, the control method as a whole is discussed in relation to the presented work and further research options.

Introduction

The grid-connected voltage-source converter (VSC) is a key technology for the integration of renewable energy sources, scalable loads, and high-performance drives in the electrical power grid [1]. Well-performing grid-connected VSCs are hence essential for the realization of a carbon-neutral energy system. Inconveniently, VSCs are nonlinear closed-loop controlled switching devices that inherently inject unwanted frequency content into the grid, thereby affecting other equipment and in some cases exciting the grid system resonances to cause instability problems.

Third-order LCL-filters are commonly used between the point-of-common-coupling (PCC) of the grid and the VSC to minimize these effects [2]. The objective of current control for LCL-filtered VSCs is complicated by the instability which is introduced by the digital control delay and converter switching action, coupled with the natural resonance frequency of the filter and grid impedance. This poses both hardware constraints and control challenges for the power electronic design procedure. In grid-connection applications, the converter must adhere to grid-codes regarding steady-state performance with tracking of the fundamental for current injection and limits to unwanted harmonics into the grid. Specifications to the performance during transients further complicates the design procedure and additionally, a stable and robust design is needed to cope with parameter uncertainty and variations.

Current control is commonly done with linear PI controllers in the synchronous reference frame or PR controllers in the stationary reference frame, both including a fixed switching frequency Pulse Width Modulator (PWM). Addressing the issue of the LCL-filter resonance can be achieved by reaching a design which avoids this issue altogether, by strategically placing the switching and filter self-resonance frequencies. However, the filter resonance is also affected by the equivalent grid impedance and is therefore subject to change during operation, which futher complicates the robust design procedure. Another option is to dampen the resonance. This can be done by passive damping, active damping or hybrid damping. The passive damping involves placing a physical resistor within the filter, either in connection with the inductors or capacitor [3]. Although this method is robust and reliable, it introduces power loss in the system. Therefore, active damping, by means of control efforts is often a preferred solution that has been explored by numerous researchers in the last decade [4]. Indeed, a rich body of literature is available [5],[6],[7], which state-of-the-art commercial microprocessors and integrated circuits can easily implement.

To improve on state-of-the-art, an ideal current controller should adjust the converter's switching according to the operating conditions: fast actuation during transients and simultaneously provide tailored and optimized performance in steady-state, while setting a minimum of requirements to the hardware. This means that the controller should operate with a high bandwidth, to offset the physical limitations of the hardware and push the converter performance to the limit. A such controller is proposed in this paper.

Proposed Method

As previously mentioned, the resonance problem that arises with LCL filtered two-level VSCs (2L-VSC) is mainly caused by the resonance interaction between the filter capacitor and inductors, which are being excited by the switching action of the converter. To remedy the problem, this paper proposes a solution where the dynamics of the LCL-filter are decoupled by the Finite Control Set (FCS) Model Predictive Control (MPC) which generate the voltage reference on the filter capacitor. By doing so, within the bandwidth of the MPC, the VSC and the LC part of the filter can be treated as an ideal controlled voltage source. Thus, the current control problem can be reduced to a plant consisting only of the grid-side filter inductor and grid impedance, which among different methods, can be controlled by a Proportional-Resonant (PR) controller in the stationary reference frame [8],[9].

The feasibility of this method is greatly enhanced by the improved voltage tracking performance of the FCS-MPC algorithm, reported in [10]. Here, a continuity of the controlled state derivative is added to the cost function. This has the benefit of reducing the output voltage Total Harmonic Distortion (THD) and thereby improving the approximation as an ideal 50 Hz voltage source.

The voltage reference, provided by the PR controllers, is actuated by the FCS-MPC algorithm by selecting the switching state which minimizes a predefined cost function at every sampling instance. In this way, the variable switching frequency MPC replaces the fixed switching frequency Pulse Width Modulator (PWM). This algorithm is briefly summarized here.

First, a state-space model of the observed states can be formulated as

$$\frac{d}{dt}\begin{bmatrix} i_f \\ v_f \end{bmatrix} = \mathbf{A}\begin{bmatrix} i_f \\ v_f \end{bmatrix} + \mathbf{B}\begin{bmatrix} v_i \\ i_g \end{bmatrix}, \tag{1}$$

where i_f, v_f, v_i, and i_g are the converter current, capacitor voltage, converter voltage, and grid current, respectively. All quantities are complex vectors in the stationary reference frame. Here, the state-space matrices represent the LC filter dynamics:

$$\mathbf{A} = \begin{bmatrix} -\frac{R_f}{L_f} & -\frac{1}{L_f} \\ \frac{1}{C_f} & 0 \end{bmatrix}, \tag{2}$$

$$\mathbf{B} = \begin{bmatrix} -\frac{1}{L_f} & 0 \\ 0 & -\frac{1}{C_f} \end{bmatrix}, \tag{3}$$

where L_f, R_f, and C_f are the converter side filter inductance, associate Equivalent Series Resistance (ESR) and filter capacitance, respectively. The state-space model is discretized using a Zero Order Hold (ZOH) for the digital implementation.

The first step is to acquire measurements of all state variables and convert them from the natural reference frame to to the stationary reference frame. Thereafter, the measurements are fed to the MPC algorithm where the stored knowledge about the previously applied switching states are used, in conjunction with the state-space model, in order to compensate any system time delays (sampling and transport delays). The second step is to evaluate each possible switching state of the 2L-VSC using a cost function to determine which state should be applied in the subsequent switching period. The Cost Function (CF) used for this implementation is

$$CF = g_{con} + \lambda_d g_{der} + h_{lim} + \lambda_u sw^2, \tag{4}$$

where g_{con} is the Euclidean distance between the reference vector and the measured capacitor voltage expressed as

$$g_{con} = (v^*_{f\alpha} - v_{f\alpha})^2 + (v^*_{f\beta} - v_{f\beta})^2. \tag{5}$$

To improve the steady-state performance of the MPC, a term which tracks the derivative of the voltage reference is included in the CF. This is as proposed in [10] and is expressed as,

$$g_{der} = (C_f \omega_n v^*_{f\beta} - i_{f\alpha} + i_{g\alpha})^2 + (C_f \omega_n v^*_{f\alpha} + i_{f\beta} - i_{g\beta})^2, \tag{6}$$

where ω_n is the nominal angular grid frequency. Alternatively, to allow the MPC to take into account grid frequency variations, ω_n can be obtained from the estimated frequency of the PLL. Tuning of the CF can be done through the weights, λ_d and λ_u, which penalize the different terms included in the CF. To protect the converter from over current and short circuit situations, h_{lim} is set to infinity if the magnitude of the converter current exceeds a predefined maximum value, i.e. dominating the CF and dictating the switching state. At all other times the limit term is reduced to zero, effectively eliminating its effect on the CF. After the state variables are measured, the discrete time model of the output filter and 2L-VSC is used to calculate the future propagations for each possible switching state. The switching state which minimizes the CF is then selected and applied in the next switching instance.

A combined block diagram of the converter power stage schematic and control block diagram is shown in Fig. 1, where the MPC takes the place of the PWM and active damping in a conventional linear control scheme. Since the MPC algorithm is based on a state-space model of the system, time delays are also easily compensated [10],[11] to further increase the potential control bandwidth.

The current reference generation and tracking of the grid voltage is realised using a Synchronous Reference Frame (SRF) Second Order Generalised Integrator (SOGI) Phase-Locked Loop (PLL) [12]. The

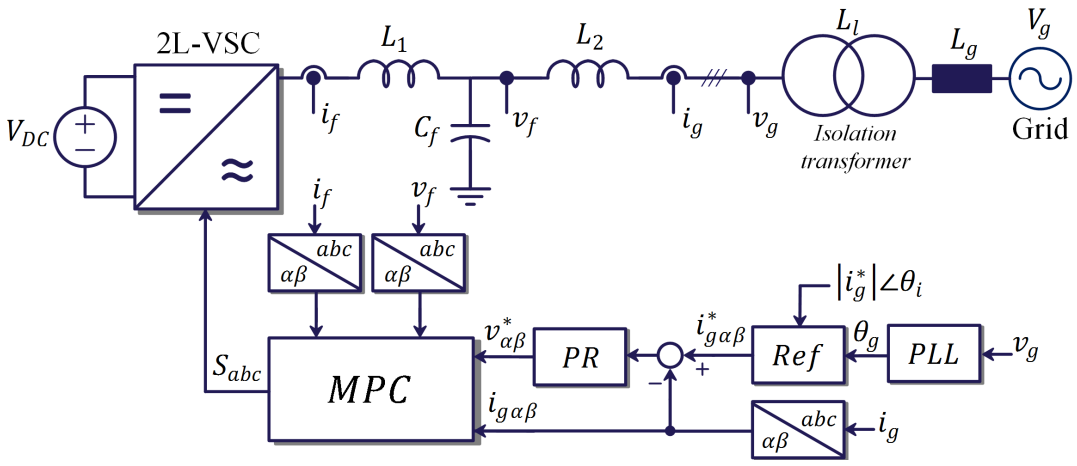

Fig. 1: Schematic overview of the converter power stage and control blocks, including the MPC algorithm, PR controller and PLL.

SOGI, prior to the SRF-PLL, acts as a second-order bandpass filter which only tracks the fundamental component of the grid voltage and attenuates all other frequencies present in the grid voltage. In this way, the PLL is able to accurately synchronize to the fundamental frequency phase. The SOGI SRF-PLL considered in this paper, is depicted in Fig. 2.

To generate the capacitor voltage reference sent to the MPC, based on a reference value for the grid current, a current regulator is implemented as a outer linear controller forming a hybrid control solution with an inner nonlinear voltage controller and an outer linear current controller. The linear current controller is usually implemented as a PI controller in the synchronous dq-reference frame or as a PR controller in the stationary αβ-reference frame. Certain advantages exists when employing a PR controller compared to a PI controller in the synchronous reference frame. The PR controller is inherently capable of compensating both positive and negative sequence component frequencies which, if implemented in the synchronous reference frame, takes two PI controllers for each fundamental. Secondly, by using PR controller in comparison to PI controller the grid phase angle estimated with the SOGI SRF-PLL is not coupled to more control loops than necessary. Due to this and since the reference values fed to the MPC algorithm are expressed in the stationary αβ reference frame a PR controller with harmonic compensation is used to achieve zero steady-state error in the injected grid currents [13]. The transfer function of the PR controller is

$$G_{PR}(s) = K_p + K_i \sum_h \frac{s \cdot \cos(\phi_h) - h\omega_n \cdot \sin(\phi_h)}{s^2 + (h\omega_n)^2} \tag{7}$$

where h is the targeted harmonic, including $h = 1$ for the fundamental component at ω_n. The addition of

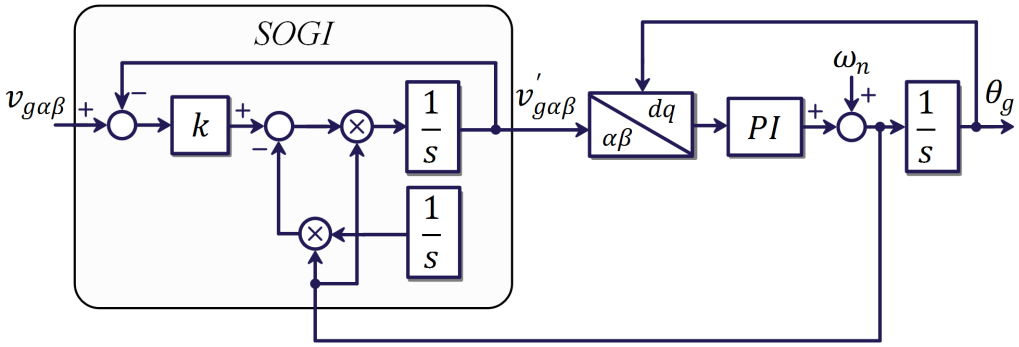

Fig. 2: Structure and implementation of SOGI SRF-PLL which is implemented as the synchronization unit for the MPC reference generation.

$\phi_f = h\omega_f T_s$, is made to compensate the phase at the resonance frequency and thereby reducing the instability caused by the sample time delay [14]. The proposed hybrid controller structure for a grid-connected converter has been described and each control block has been carefully explained. The subsequent sections consider the tuning procedure of the hybrid controller, performance of proposed controller, and experimental verification conducted to verify the simulation studies and analytical design.

Table I: Experimental parameters for the converter control

Symbol	Meaning	Value
V_g	Grid voltage (line-to-line)	400 V
f_1	Grid frequency	50 Hz
f_s	Sampling frequency	50 kHz
V_{DC}	DC link voltage	800 V
L_f	Converter-side inductor	1.4 mH
L_g	Grid-side inductor	2.4 mH
L_l	Transformer inductance	1.1 mH
C_f	Filter capacitance	14 μF
i_g^*	Reference active current	15 A

Design Guidelines and Control Bandwidth

The process of selecting a set of robust control parameters for a hybrid control-scheme is challenged by the nonlinear controller dynamics. Therefore, this section is dedicated to describing some of the considerations that should be made for the design procedure.

FCS-MPC

With the inner-loop voltage controller comprised of the nonlinear FCS-MPC which regulates the ac filter capacitor voltage, the LCL-filter dynamics can be decoupled. This requires a bandwidth which is higher than the current controller, so that unstable interactions are avoided. The parameters that affect the FCS-MPC bandwidth have been found through empirical studies and experiments to be:

- DC link voltage and capacitor AC voltage operating point
- LC-filter parameters
- Sampling/switching frequency
- Cost function formulation and weights

The cost function and weights determine which state will be prioritized in any given switching instant. Therefore, this has a large impact on the control bandwidth. The switching penalty and the hard current limiter both decrease bandwidth because they allow the controller to prioritize objectives, other than regulating the desired reference voltage. The derivative term is similar to this. It is desirable to track the reference 50 Hz derivative, and this will allow the controller to reduce the high frequency currents injected into the grid, thereby reducing the THD. Contrary to this, any frequency components present in the grid will have reduced priority in the capacitor voltage, and therefore reduce the controller bandwidth. With bandwidth as a single performance metric, these weights should be minimized, but with respect to switching losses, current limitation and THD, a trade-off must be found through simulations and parameters sweeps.

The filter parameters introduce an impedance which acts against changes in voltage and current, naturally this will lower the FCS-MPC bandwidth as well. Minimizing the filter will increase the control bandwidth, but suppression of unwanted frequency content must be considered in this process, again introducing a trade-off. Increasing the sampling frequency allows the controller to detect and actuate changes faster, increasing the bandwidth. Similarly, increasing the DC link voltage, relative to the capacitor AC voltage operating point, also increases the bandwidth by providing the controller with more

influence on the filter state during a switching period. The impact of these parameters can be used during the design procedure to maximize the MPC performance.

In this paper, the weights are $\lambda_d = 3$ and $\lambda_u = 0$ with a hard current limit at 30 A. Through multiple simulation, these have been found to provide the best trade-off between THD and bandwidth, with this specific filter and control design.

PR current controller and SRF-PLL

Tuning the current controller is done with classical linear control theory and in relation to the FCS-MPC. A small-signal perturbation frequency sweep was applied to the FCS-MPC reference in the positive sequence and the response was measured. This results in figure 3, where the corresponding estimated transfer function is also shown. This is a mathematical curve fitting procedure, so the resultant pole-zero placement does not reveal any physical insights into the FCS-MPC performance. The transfer function is,

$$G_{FCS-MPC}(z) = \frac{V_c}{V_c^*} = \frac{0.01728z^{-1} - 0.006586z^{-2} + 0.1948z^{-3} + 0.06554z^{-4} - 0.1531z^{-5}}{1 - 1.454z^{-1} + 0.5564z^{-2} + 0.196z^{-3} - 0.1349z^{-4} - 0.04172z^{-5}}. \quad (8)$$

Discretization of the L-filter plant with a Zero Order Hold (ZOH), the PR controller with the pre-warped Tustin method, and adding a single sample delay yields the open-loop transfer function,

$$G_{ol}(z) = G_{PR}(z) \cdot z^{-1} \cdot G_{FCS-MPC}(z) \cdot G_{L-filter}(z). \quad (9)$$

From here, selection of the desired control parameters is a trivial procedure. As a summary of the design and dependant parameters,

- PR gains ($k_P = 25$ A/V and $k_R = 800$ A/Vs)
- Control delay ($T_d = 20\mu s$)
- MPC bandwidth ($\approx$ 7kHz)
- Equivalent L-filter plant ($2.4mH + 1.1mH = 3.5mH$)

This gives a current controller bandwidth of 2.3 kHz, which is 1/3 of the inner-loop. Thus, in this case, tuning the PR controller to achieve a bandwidth of 1/3 of that of the closed-loop inner voltage control using MPC gives a phase margin and gain margin of 45° and 7 dB, respectively. Using linear control theory the proportional gain which destabilizes the system is found to be 61.65. As it can be seen from Fig. 3, the nonlinear MPC can be closely represented by a linear transfer function. This indicates, that a linear model of the MPC may be derived with a low loss of accuracy. However, this hypothesis needs to be further investigated through multiple simulations at different operating points to reveal whether this is true. The SRF-PLL is designed to be slower than the current control loop to avoid interaction between the loops. In this case, the controller gains are set at $k_{p,PLL} = 0.2831$ Hz/V and $k_{i,PLL} = 0.0377$ Hz/Vs, which yields a bandwidth of 15 Hz.

Validation with experimental results and simulations

The proposed method was experimentally validated with the laboratory setup shown in Fig. 4. The 2L-VSC was a SEMIKRON Semiteach converter platform, based on the SKM 50 BG 123 D 3-phase IGBT module. The control was implemented with a dSPACE MicroLab Box using the DS1202 base board and DS1302 I/O board with external current (LA55-p-e) and voltage (LV25-p) sensors. The measurements were recorded with the DPO 3014 Tektronix scope, TCP 0030A current sensor and P5200 HV active differential probe for voltage measurements.

With the parameters listed in Table. I, the LCL-filter self-resonance is [15],

$$f_{res} = \frac{1}{2\pi}\sqrt{\frac{L_f + L_g + L_l}{L_f (L_g + L_l) C_f}} = 1.35kHz, \quad (10)$$

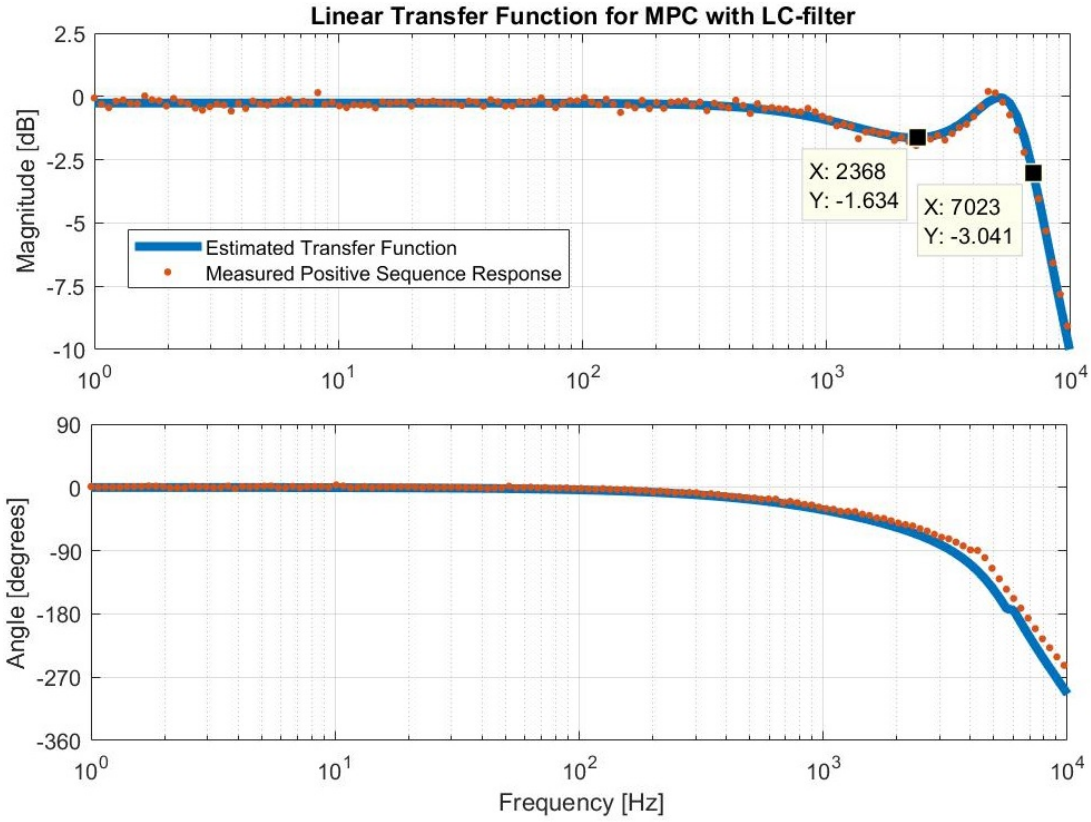

Fig. 3: Estimate of the MPC positive sequence closed-loop control transfer function.

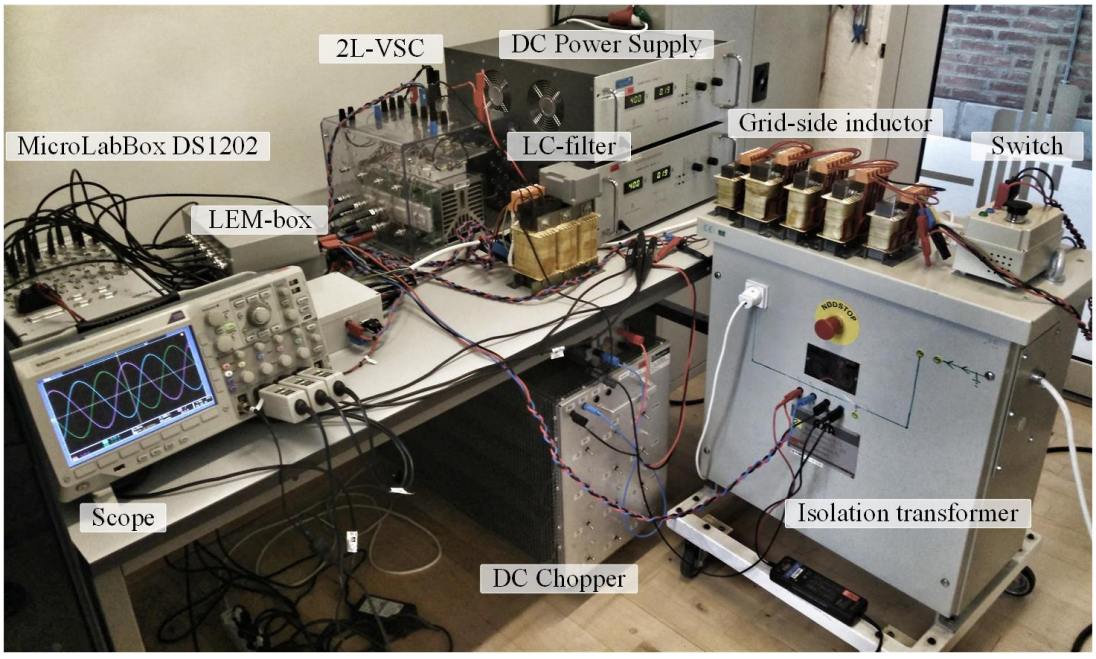

Fig. 4: Picture of the experimental set up used to validate the proposed control method in the laboratory.

where L_l is the transformer leakage inductance and equivalent grid inductance, which is approx. 1.1 mH in the setup.

Three experiments were performed: 1) with the current controller in steady state and tracking a 15 A reference, 2) a step response from 5 A to 15 A and 3) increasing the controller proportional gain until instability occurred. This was done to test the stability limit of the controller. All of these experiments were also replicated in simulation to validate a used SIMULINK model. The results are shown in Fig. 3, Fig. 4, and Fig. 5. The steady-state error is less than 1% and the THD is 1.08% in the case where the gains for the current regulator are Kp = 30 and Ki = 800. The rise-time of the step response is below 1 ms, with no overshoot and minimal oscillations. The control algorithm sampling frequency was 50 kHz. This high sampling frequency ensures a fast dynamic response of the PR-controllers and improves the MPC tracking performance while keeping the switching frequency low with the FCS-MPC. The experimental system setup parameters are summarized in Table. I. As it can be noticed from Fig. 7, the stability limit of the proportional gain closely matches what was predicted in the previously discussed linear analysis where the MPC where represented by a linear discrete transfer function.

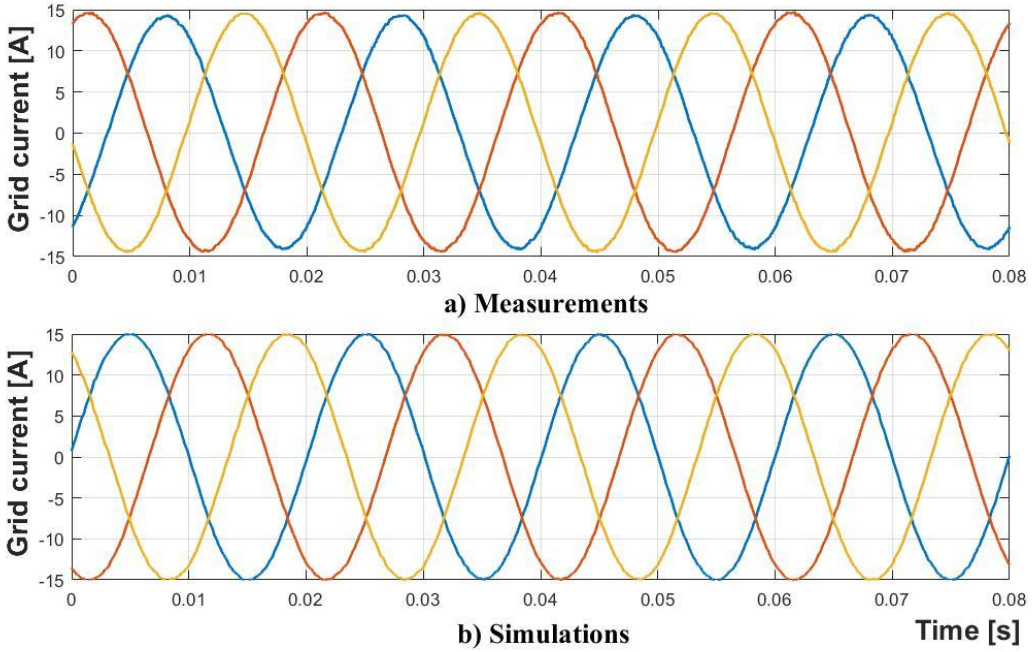

Fig. 5: Steady state results from a) experiments with THDi = 1.08% and b) simulations with THDi = 1.62%. Both results are with Kp = 30 and Ki = 800.

Conclusion

As the penetration of renewable energy sources in the power system increases, the need for high-performance control becomes more important. Therefore, this paper has proposed an algorithm that utilizes the advantages of both PLL and PR control as well as FCS-MPC to produce a hybrid control schemes which provides good steady state performance and fast dynamic response with ample margin for stability. This was done by utilizing the MPCs variable switching frequency and fast sampling to track the filter capacitor voltage, which in turn decouples the LCL filter dynamics and thereby simplifying the plant seen by the PR controller. This also removes the need for damping, since this is inherently provided by the MPC within its bandwidth. A design guideline for the hybrid controller was given where it was recommended to tune the PR controller to have a bandwidth of 1/3 of the MPC bandwidth. This resulted in a current regulator with a bandwidth above 2 kHz, easily capable of ensuring fast controller dynamics and robust performance.

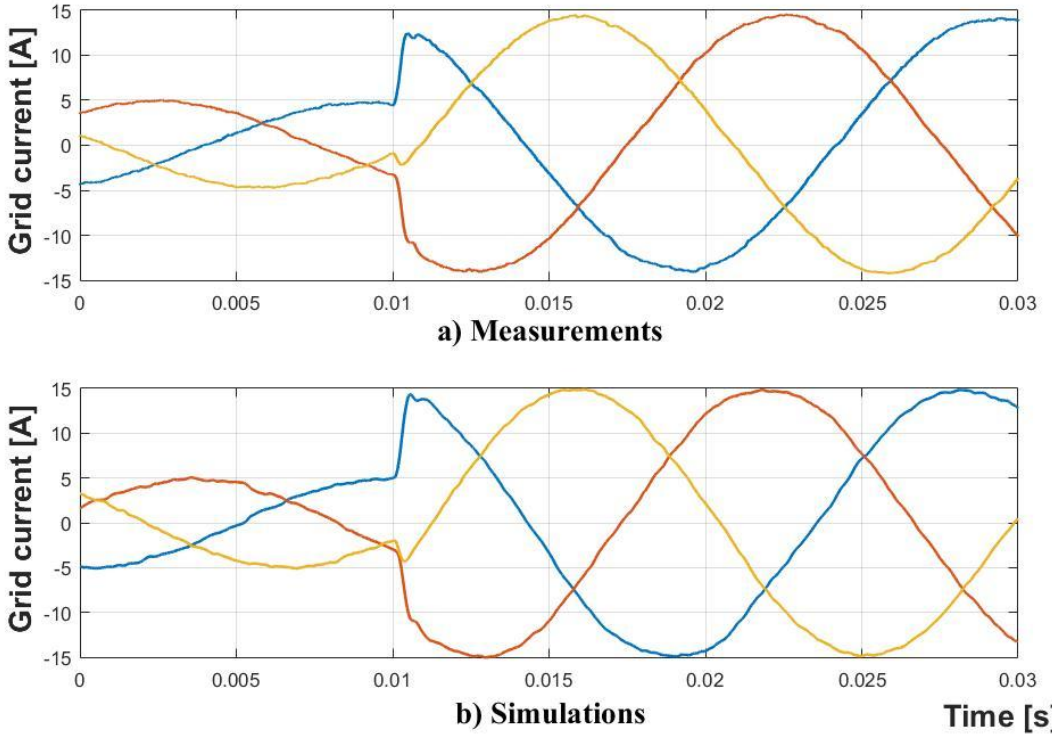

Fig. 6: Step response from a) experiments and b) simulations. The step is made from 5 A to 15 A, both with Kp = 15 and Ki = 800.

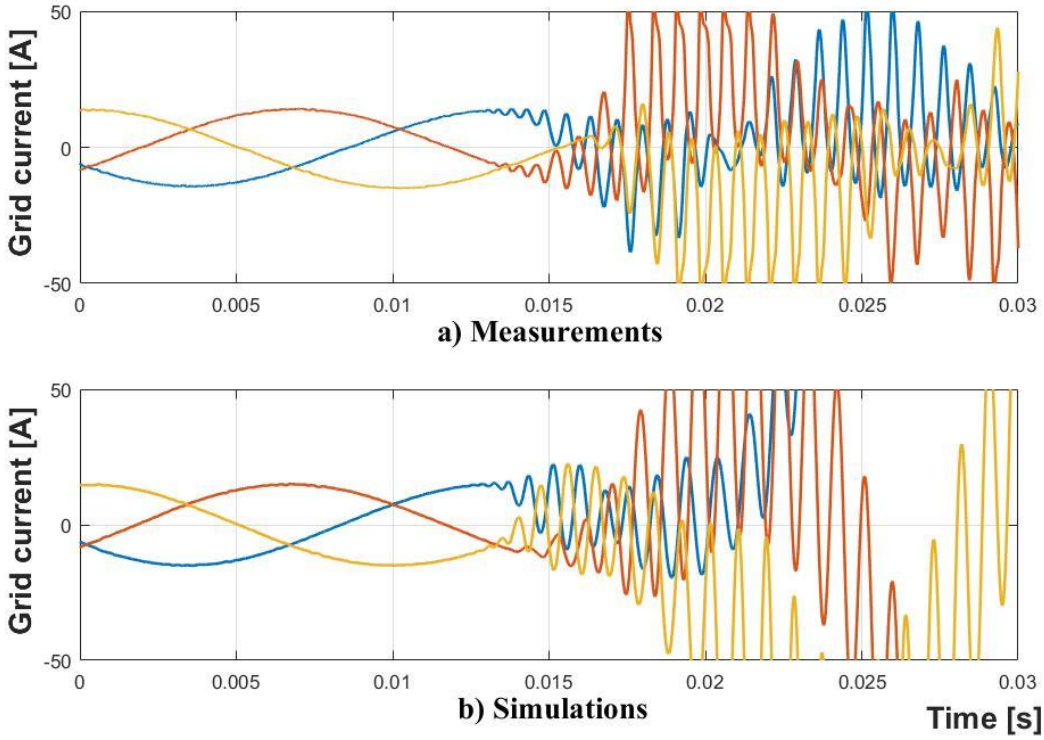

Fig. 7: Instability provoked by increasing the PR controller proportional gain a) experiments (Kp = 53.5) and b) simulations (Kp = 60.0), both with Ki = 800.

The possibility of applying FCS-MPC as a fast inner voltage control loop for added stability, damping, and control, is advantageous as it has been shown in this paper by simulations and experiments. The inherent advantages of the hybrid control method are:

1. System damping is provided by decoupling of filter dynamics
2. Fast dynamic response and variable switching frequency which ensure high performance with lower losses
3. Simultaneous multi-objective control of the THD, limit the current or vary the average switching frequency
4. Easy compensation of system delays and nonlinearities

For present and future high power converters where the control performance is crucial and the added cost of additional sensors and computational power is insignificant, compared to system costs, this method could easily be applied.

However, further work is needed to fully utilize this method. This includes analytically studying and predicting the control performance of the hybrid control method during the design phase and addressing the untoward effects, such as:

1. Higher computational burden compared to pure linear control
2. Faster sampling frequency to further improve performance
3. Additional sensors or state observers which can increase costs or complicate the control
4. Variable switching frequency which results in harmonics across the frequency spectrum
5. Control performance is linked to model accuracy, which can degrade performance as the system changes

References

[1] F. Blaabjerg, Z. Chen and S. B. Kjaer, Power Electronics as efficient interface in dispersed power generation systems, in IEEE Transactions on Power Electronics, vol. 19, no. 5, pp. 1184-1194, 2004.

[2] R. Narcis, X. Wang, M. Liserre, F. Blaabjerg and C. L. Bak, A Review of Passive Power Filters for Three-Phase Grid-Connected Voltage-Source Converters, in IEEE Journal of Emerging and Selected Topics in Power Electronics, vol. 4, no. 1, pp. 54-69, 2016.

[3] R. N. Beres, X. Wang, M. Liserre, F. Blaabjerg and C. L. Bak, A Review of Passive Power Filters for Three-Phase Grid-Connected Voltage-Source Converters, in IEEE Journal of Emerging and Selected Topics in Power Electronics, vol. 4, no. 1, pp. 54-69, March 2016.

[4] W. Wu, Y. Liu, Y. Hu, H. S.-H. Chung, M. Liserre and F. Blaabjerg, Damping Methods for Resonances Caused by LCL-Filter-Based Current-Controlled Grid-Tied Power Inverters: An Overview, in IEEE Transactions on Industrial Electronics, vol. 64, no. 9, pp. 7402-7413, September 2017.

[5] J. Wang, J. D. Yan and L. Jiang, Pseudo-Derivative-Feedback Current Control for Three-Phase Grid-Connected Inverters With LCL Filters, in IEEE Transactions on Power Electronincs, vol. 31, no. 5, pp. 3898 - 3912, May 2016.

[6] I. Lorzadeh, M. Savaghebi, H. A. Abyaneh and J. M. Guerrero, Active damping techniques for LCL-filtered inverter-based microgrids, in IEEE 10th International Symposium on Diagnostics for Electrical Machines, Power Electronics and Drives, pp. 408-414, 2015.

[7] D. Pan, X. Ruan, X. Wang, H. Yu and Z. Xing, Analysis and Design of Current Control Schemes for LCL-Type Grid-Connected Inverter Based on a General Mathematical Model, in IEEE Transactions on Power Electronics, vol. 32, no. 6, pp. 4395-4410, 2017.

[8] S. G. Parker, B. P. McGrath and D. G. Holmes, Regions of Active Damping Control for LCL Filters, in IEEE Transactions on Industry Applications, vol. 50, no. 1, pp. 424-432, 2014.

[9] B. Li, W. Yao, L. Hang and L. M. Tolbert, Robust proportional resonant regulator for grid-connected voltage source inverter (VSI) using direct pole placement design method, in IET Power Electronics, vol. 5, no. 8, pp. 1367-1373, 2012.

[10] T. Dragicevic, Model Predictive Control of Power Converters for Robust and Fast Operation of AC Microgrids, in IEEE Transactions on Power Electronics, vol. PP, no. 99, pp. 1-1, November 2017.

[11] P. Cortes, J. Rodriguez, C. Silva and A. Flores, Delay Compensation in Model Predictive Current Control of a Three-Phase Inverter, in IEEE Transactions on Industrial Electronics, vol. 59, no. 2, pp. 1323-1325, 2012.

[12] P. Rodriguez, A. Luna, R. S. Munoz-Aguilar, I. Etxeberria-Otadui, R. Teodorescu and F. Blaabjerg, A Stationary Reference Frame Grid Synchronization System for Three-Phase Grid-Connected Power Converters Under Adverse Grid Conditions, in IEEE Transactions on Power Electronics, vol. 27, no. 1, pp. 99-112, January 2012.

[13] R. Teodorescu, F. Blaabjerg and M. Liserre, Proportional-Resonant Controllers. A New Breed of Controllers Suitable for Grid-Connected Voltage-Source Converters, in Proceedings of the 9th International Conference on Optimization of Electrical and Electronic Equipment, vol. 3, pp. 9-14, 20-22 May 2004.
[14] A. G. Yepes, F. D. Freijedo, O. Lopez and J. Doval-Gandoy, Analysis and Design of Resonant Current Controllers for Voltage-Source Converters by Means of Nyquist Diagrams and Sensitivity Function, in IEEE Transactions on Industrial Electronics, vol. 58, no. 11, pp. 5231-5250, November 2011.
[15] Z. Xin, X. Wang, P. C. Loh and F. Blaabjerg, Grid-Current-Feedback Control for LCL-Filtered Grid Converters With Enhanced Stability, in IEEE Transactions on Power Electronics, vol. 32, no. 4, pp. 3216-3228, April 2017.